# Independent Tuning of the Band Gap and Redox Potential of Graphene Quantum Dots

**ARTICLE** *in* JOURNAL OF PHYSICAL CHEMISTRY LETTERS · APRIL 2011

Impact Factor: 7.46 · DOI: 10.1021/jz200450r



**6 AUTHORS**, INCLUDING:

Binsong Li
Sandia National Laboratories
**27** PUBLICATIONS **1,203** CITATIONS
SEE PROFILE

Qingshuo Wei
National Institute of Advanced Industrial Sci…
**33** PUBLICATIONS **1,425** CITATIONS
SEE PROFILE

Keisuke Tajima
RIKEN
**105** PUBLICATIONS **3,921** CITATIONS
SEE PROFILE

THE JOURNAL OF PHYSICAL CHEMISTRY Letters

LETTER

pubs.acs.org/JPCL

# Independent Tuning of the Band Gap and Redox Potential of Graphene Quantum Dots

Xin Yan,[†,§] Binsong Li,[†,§] Xiao Cui,[†] Qingshuo Wei,[‡] Keisuke Tajima,[‡] and Liang-shi Li*[,†]

[†]Department of Chemistry, Indiana University, Bloomington, Indiana 47405, United States

[‡]Department of Applied Chemistry, Graduate School of Engineering, The University of Tokyo, 7-3-1 Hongo, Bunkyo-ku, Tokyo 113-8656, Japan

Supporting Information

**ABSTRACT:** The band gap and redox potential of semiconductor nanocrystals are two quantities of primary importance for their applications in energy conversion devices. Herein, we report on covalent functionalization of colloidal graphene quantum dots through a solution-chemistry approach and studies of their band gaps and redox potentials. We show that their band gaps and redox potentials can be independently controlled, the former by size and the latter by functionalization. The size and the functionalization dependence of the properties can be numerically reproduced with tight-binding calculations, which thus provides a simple theoretical tool to guide the design of graphene QDs with desired properties.

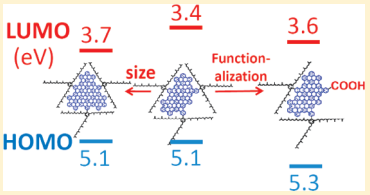


**SECTION:** Nanoparticles and Nanostructures

The size and shape dependence of electro-optical properties is a hallmark of quantum-confined systems. In colloidal semiconductor nanocrystals, the versatile tunability of properties, together with solution processability, has led to various practical applications.[1−11] While for optical applications the band gap of the nanocrystals is a primary quantity, for applications involving conversion between energies of different forms, the redox potential of the nanocrystals is another essential parameter. For example, in photovoltaic devices[6−8] or light-emitting diodes,[9−11] the energy levels in the nanocrystals relative to those of other active components determine not only the direction of charge-transfer processes but also the kinetics and efficiency. Therefore, in order to control both the flow of charges in the devices and the light that they absorb or emit, it is desirable to tune the band gaps and the redox potentials of the nanocrystals independently.

Recent studies have shown that the redox potentials of conventional semiconductor nanocrystals, such as those made of CdSe, CdS, or InAs, can be varied by changing surface ligands, independent of their band gaps that are tuned by size.[12−14] By analogy to bulk semiconductors, the potential shifting is generally believed to be due to the dipole moments of the ligands generating an electric field near the surfaces; yet at times, it can be unpredictable.[12] Herein, we report on covalent functionalization of colloidal graphene quantum dots (QDs) with a solution-chemistry approach and studies of their band gaps and redox potentials. With optical absorption spectroscopy and photoelectron spectroscopy, we show that these two important parameters can be independently controlled, the former by size and the latter by functionalization. Both the size and the functionalization dependence of the properties can be numerically reproduced with tight-binding (TB) calculations, thus providing a simple, theoretical tool to guide the future design of graphene QDs with desired properties.

Colloidal graphene quantum dots (QDs) are a new type of quantum-confined system that we recently introduced as light absorbers in photovoltaic devices.[15,16] Made through stepwise organic chemistry routes from small organic molecules, they have properties resembling more nanocrystalline solids than molecules. For example, the graphene QDs have continuous absorption spectra in the UV−visible region due to the overlap of electronic absorption bands caused by closely spaced electronic energy levels and vibronic coupling.[16,17] The graphene QDs were also shown to have very slow hot-carrier cooling dynamics,[18] reminiscent of the "phonon bottleneck" that was intensively investigated in conventional semiconductor quantum dots.[19] Because they are made of abundant elements on earth and contain no rare or toxic metal, the graphene QDs are attractive for various energy-related applications. Further, comparing with the most widely studied light absorbers for solar energy conversion such as ruthenium complexes and inorganic quantum dots, graphene QDs have some superior properties including much greater extinction coefficients than the ruthenium complexes[16] and band gaps tunable, in principle, to as small as 0 eV. The extraordinarily long lifetimes of hot carriers[18] could potentially allow for hot-carrier transfer or multiexciton generation that could overcome the Shockley−Queisser limit in solar energy utilization.[20,21]

Functionalization of graphene QDs is a crucial step toward improving their performance in energy conversion devices

**Received:** April 4, 2011
**Accepted:** April 18, 2011
**Published:** April 22, 2011

because it controls the interaction between the QDs and the other active components in the devices. For the QDs to be used as sensitizers in dye-sensitized solar cells, for example, as revealed with many other sensitizer systems,[22−25] chemical functionalization, especially with surface-binding groups, not only determines their surface coverage on semiconducting oxides but also plays an important role in dictating the photoinduced charge injection. In addition, defects in graphitic carbon with various functionalities are widely believed to be responsible for the activities of various carbon materials used in catalysis, in particular, for reactions normally requiring rare metals.[26−28] Therefore, studies of well-defined, functionalized graphene QDs could shed light on the mechanisms in the complex systems and possibly lead to rational improvement of their functions.

In this work, we have studied graphene QDs **1**−**6** (Scheme 1). The QDs were synthesized with solution-chemistry routes similar to what we previously developed to obtain **1** and **2** from small aromatic compounds.[17] To illustrate this solution-chemistry approach, we summarize the synthesis of QDs **3** and **4** in Schemes 2 and that of QDs **5** and **6** in the Supporting Information. For all of the QDs, we started with synthesizing polyphenylene dendrimeric precursors (e.g., **12** and **13** in Scheme 2) and subsequently oxidized them to form the graphene QDs. All of the precursors have the solubilizing 2′,4′,6′-trialkyl-substituted phenyl groups preinstalled to prevent the graphene QDs from aggregating as soon as they are made. The trialkyl-substituted phenyl groups twist from the plane of the graphene due to the crowding on the edges, resulting in the alkyl chains spanning a three-dimensional cage that prevents the graphene QDs from approaching each other.[16]

While all of the reaction intermediates to the graphene QDs were purified with silica gel chromatography and confirmed with standard characterization methods (see Supporting Information), due to dynamic aggregation of the graphene QDs in solution and their high rigidity,[15,16] we were not able to detect the aromatic protons with conventional liquid-phase NMR spectroscopy even at elevated temperatures.[15,16] As a result, the graphene QDs were identified with isotope-resolved MALDI-TOF mass spectroscopy (MS) (Figure 1), which has been the only applicable method for ensemble characterization of large graphene nanostructures.[15−17] By comparing the experimental spectra with simulated ones, we could identify the targeted QDs to be the predominant species in the final products. Meanwhile, the MS spectra also indicated the presence of a small amount of mono- or dichlorinated products as well as partially oxidized ones. Neither normal-phase nor reverse-phase chromatography techniques were able to remove the impurities from the QDs,[15] and therefore, the QDs were used for subsequent studies without further purification. However, as discussed below, it is possible to exclude the contribution of the impurities with spectroscopic techniques that selectively interrogate the QDs with desired structures. Further, in the case of **6**, because of the

**Scheme 1. Molecular Structures of Graphene Quantum Dots (QDs) 1−6**

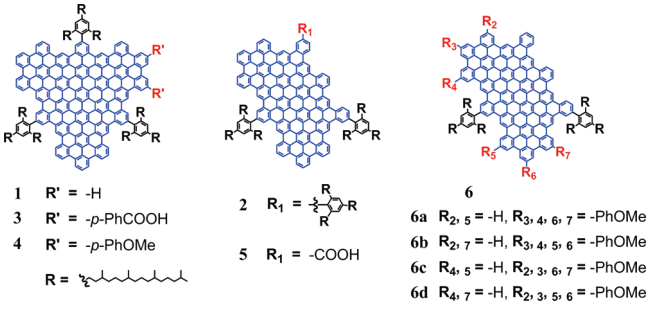


**Scheme 2. Synthesis of Graphene QDs 3 and 4**[a]

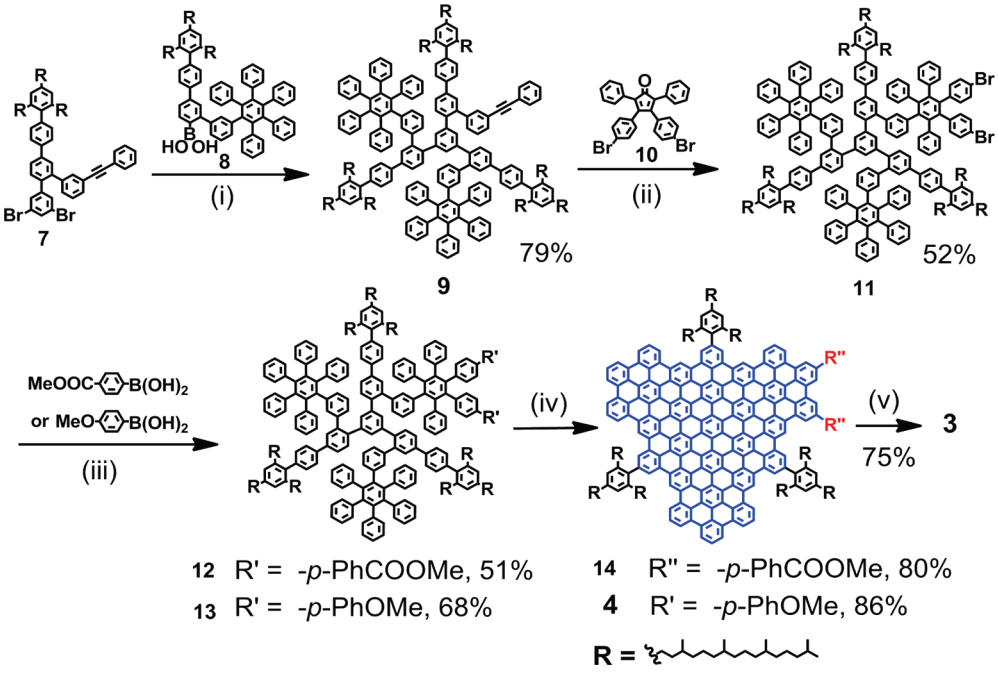


[a] Conditions: (i) $Pd(PPh_3)_4$, $K_2CO_3$, toluene, EtOH, $H_2O$, 80 °C; (ii) diphenyl ether, reflux; (iii) $Pd(PPh_3)_4$, $K_2CO_3$, toluene, MeOH, $H_2O$, 80 °C, 4-methoxycarbonylphenylboronic acid for **12** and 4-methoxyphenylboronic acid for **13**; (iv) $FeCl_3$, $CH_2Cl_2$, $CH_3NO_2$; (v) (with **14**) $BBr_3$, $CH_2Cl_2$, 0 °C.


dx.doi.org/10.1021/jz200450r |J. Phys. Chem. Lett. 2011, 2, 1119–1124

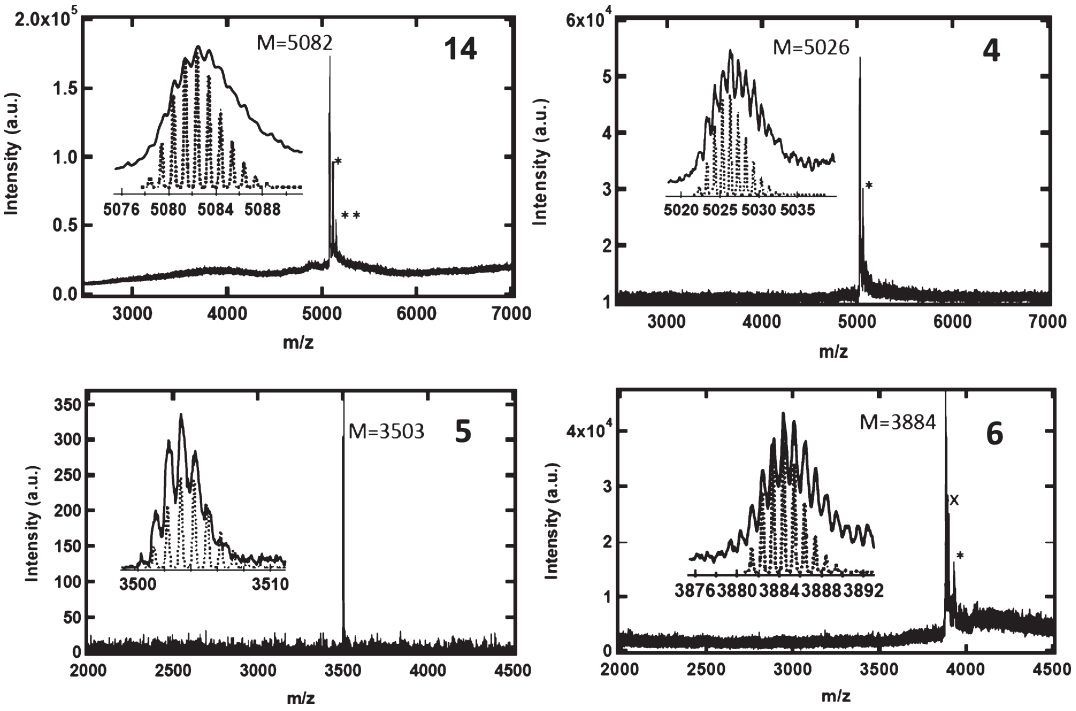


**Figure 1.** MALDI-TOF MS spectra of quantum dots **14** (methylated precursor of **3**) and **4**−**6**. In the insets are the isotope-resolved patterns experimentally observed (solid curves) with ones calculated (dotted curves) from the molecular structures. In the spectra of **14**, **4**, and **6**, the peaks marked by an asterisk are due to monochlorinated byproducts (M+34), and the one marked by two asterisks is due to dichlorinated byproducts (M+68) in the last oxidation step. In the case of **6**, the peak marked by an "x" corresponds to M+12, probably partially oxidized products. MALDI-MS spectra for **3** were not able to achieve isotope resolution for unknown reasons (see Supporting Information) but were sufficient to confirm the conversion of the methyl esters (**14**) to free carboxylic acids (**3**).

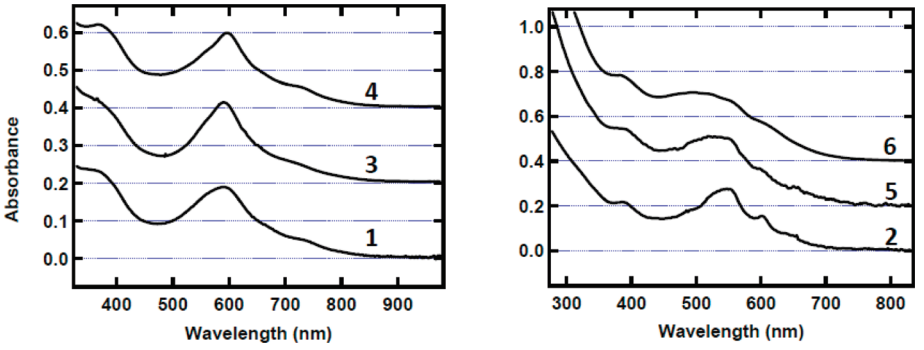


**Figure 2.** UV−vis spectra of graphene QDs **1**−**6** in toluene. **1**, **3**, and **4** have equal absorption edges at ∼900 nm, and **2**, **5**, **6** have equal absorption edges at ∼760 nm.

multiple conformation of the precursor (**27** in the Supporting Information), the resultant oxidation product **6** is a mixture of four isomers (**6a**−**d**). No further attempts were made to separate them either because they are likely to have similar optical and electronic properties.

The gaps between the highest occupied molecular orbitals (HOMO) and the lowest unoccupied molecular orbitals (LUMO) (i.e., band gaps) of the graphene QDs **1**−**6** were determined with UV−vis absorption spectra (Figure 2). In all cases, the spectra appear continuous because of vibronic broadening and the small energy spacing between the excited electronic states.[17] The band gaps were determined by the red edge of the absorption spectra, which for **1**, **3**, and **4** are ∼1.4 eV (∼ 900 nm) and for **2**, **5**, and **6** are ∼1.6 eV (∼760 nm). As expected, the QDs with 168 conjugated carbon atoms (**1**, **3**, and **4**) have smaller band gaps than those with 132 conjugated carbon atoms (**2**, **5**, and **6**) due to their larger size of conjugation. While the band gaps are dependent on the sizes of the graphene moieties, the effect of the covalent functionalization on the band gaps is not significant. The functionalization only varies the relative intensities of the finer features that correspond to different absorption bands.[17] This can be attributed to the change in the oscillator strengths of the electronic transitions due to the different electron distribution in the graphene moieties as well as the reduced molecular symmetry. In the spectrum of **6**, the transition bands are not as distinct probably because of the existence of various isomers.

Because the graphene QDs are extensions of polycyclic aromatic hydrocarbons, we anticipate that, as in other conjugated systems, covalently attaching electron-withdrawing or -donating

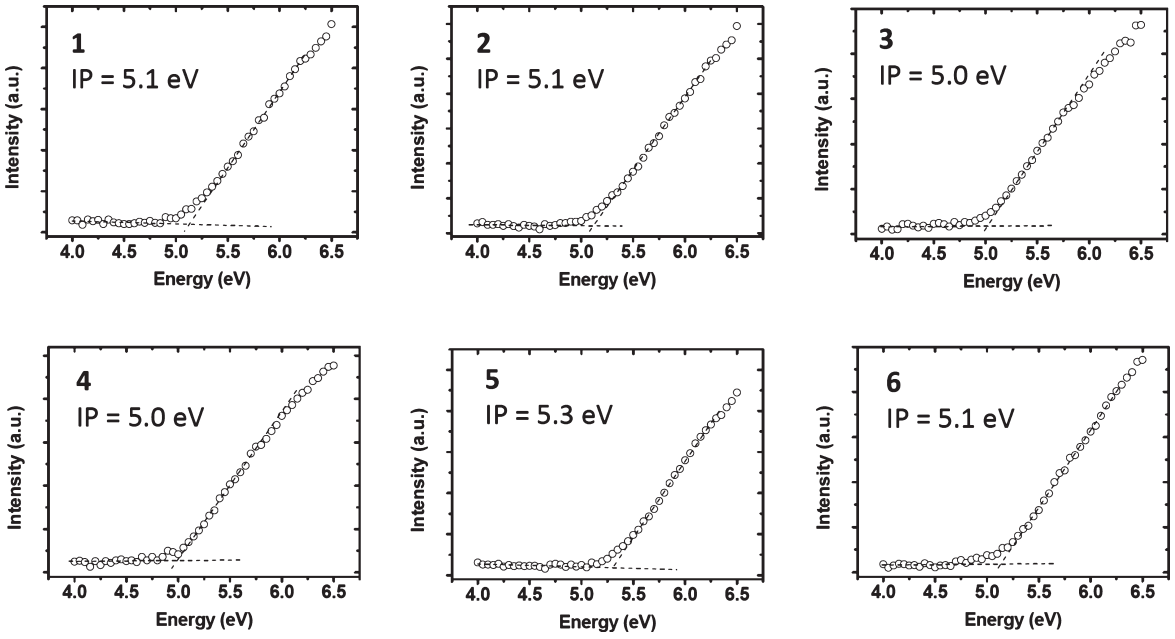


**Figure 3.** HOMO levels of graphene QDs **1**−**6** measured as the ionization potential (IP) with photoelectron yield spectroscopy (PYS). The ionization threshold was determined by extrapolating the rising edges of the spectra to cross with the tangential of the base lines.

groups should vary their redox potentials. In systems like conjugated polymers, it has been demonstrated that electron-donating groups generally raise the HOMO levels, and electron-withdrawing groups lower the LUMO levels.[29] This unique feature in the graphene QDs is of great importance for applications involving conversion between the energy of different forms because it would allow us to tune the energetics and dynamics of charge transfer independent of the band gaps.

The HOMO levels of the graphene QDs were determined as the ionization threshold energy with ultraviolet (UV) photoelectron yield spectroscopy (PYS) in air[30,31] because our attempts with cyclic voltammetry of the QDs in solution were not successful.[16] For the PYS measurements, a thin film (∼50 nm thick) of the QDs was spin-cast on an ITO-coated glass surface from a toluene solution. After it was completely dried, it was mounted in the spectrometer. UV radiation from a deuterium lamp after going through a monochromator was focused on the film, and photoelectrons emitted from the film were detected with an open counter. With photon energy increased with an interval of 0.05 eV, the photoelectron counts were measured, leading to a photoelectron spectrum. The ionization threshold energy was determined from the onset of detected electrons (Figure 3), yielding the HOMO levels of the QDs below the vacuum level in electron volts. The LUMO levels of the QDs were subsequently determined from their HOMO levels, and the band gaps were determined with UV−vis absorption spectra (Figure 2). The HOMO and LUMO levels of QDs **1**−**6** are summarized in figure 4.

It is apparent that covalent functionalization varies HOMO and LUMO levels of the graphene QDs without significantly changing their band gaps. Directly attaching the carboxylic acid group to the graphene moiety, as in the case of **5**, has the most significant effect, lowering the HOMO levels of the QDs by 0.2 eV in comparison with the nonfunctionalized **2**. The HOMO levels of both **3** and **4** were determined to be 5.0 eV below vacuum, 0.1 eV higher than that of the nonfunctionalized **1**.

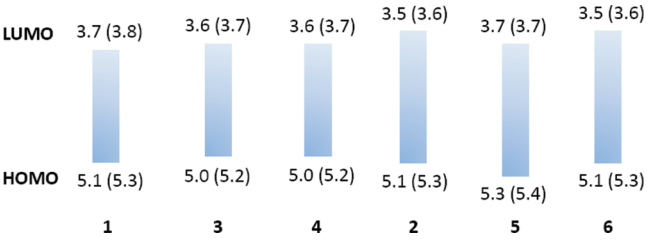


**Figure 4.** HOMO and LUMO levels of graphene QDs **1**−**6** obtained experimentally. For comparison, the values calculated with the TB model (see below) are listed in the parentheses. All of the values are in eV below the vacuum level.

Because **3** has electron-withdrawing groups and **4** electron-donating ones, the equal HOMO levels of the two suggest that the intermediate phenyl groups between the functional groups and the graphenes reduce the effects of the functionalization. This is consistent with the HOMO level of **6**, which, despite the presence of multiple methoxy groups, has the same value as the nonfunctionalized QD **2**. We have not been able to directly attach electron-donating groups such as methoxy or amine groups to the graphene moieties because of formation of quinones[32,33] or radical cations at the nitrogen centers,[34] as have been observed in smaller conjugated systems such as hexa-*peri*-hexabenzocoronene derivatives.

The effects of impurities in the QDs on the energy level determination are worth a note. From MALDI-MS, it is apparent that the most likely impurities present are chlorinated byproducts or partially oxidized ones (Figure 1). Because of the electron-withdrawing nature of the chlorine atoms, we anticipate that the chlorinated products have lower HOMO levels and therefore would not interfere with the determination of the HOMO levels that were obtained from the low-energy edges in the PYS. Similarly, partially oxidized products have larger band gaps and lower HOMO levels as well. Therefore, the determination of the

HOMO and LUMO levels from the edges of the PYS and UV−vis spectra, respectively, has an effect of spectral selection as the spectroscopic methods widely used in studying QDs of other semiconductors where a finite size inhomogeneity is always present.[35]

We compared the HOMO−LUMO levels of QDs **1**−**6** obtained experimentally with those calculated with the TB model[36] to evaluate the numerical accuracy of the latter. This work was motivated by the need for a theoretical tool to guide future development of graphene QDs without resorting to more sophisticated computation methods that are costly in calculating molecules with the size of QDs **1**−**6**. It was also encouraged by our recent work in calculating the levels of QD **1** with the TB model, which led to a mere 0.1 eV difference in band gap from the experimental value.[16]

To account for the functional groups attached to the graphene moieties, we included the heteroatoms in the TB calculation following a well-established parametrization scheme in Hückel molecular orbital theory.[37] More specifically, in the calculation, we only considered the $p_\pi$ orbitals of the carbon and oxygen atoms. To calculate the matrix elements needed, we assumed the graphene moieties to be planar and only considered the nearest-neighbor coupling. The Coulomb integral ($\alpha$) for the carbon atoms was chosen to be −4.5 eV below vacuum level, the Fermi level of bulk graphene. The transfer integral (or resonance integral, $\beta$) and overlap integral ($S$) between all of the C═C linkage were taken as −3.033 eV and 0.129, respectively, values that reproduce ab initio calculation results of graphite band structures.[36] For the oxygen atoms in C−O single bonds, the Coulomb integral was chosen to be −10.566 eV, and the transfer integral was −3.033 eV.[37] For the oxygen atoms in C═O double bonds, the Coulomb integral was −7.533 eV, and the transfer integral was −2.426 eV.[37] The overlap integral for both types of oxygen atoms was taken to be 0 (Hückel approximation). In the calculations, the electronic coupling between the graphene moieties and the solubilizing trialkylphenyl groups was ignored because of the out-of-plane configuration between the two.

Following a standard procedure,[36] we solved for the eigenenergy of the single-electron orbitals, as listed in Figure 4, for QDs **1**−**6**. The calculated results not only agree very well with the experimentally measured HOMO and LUMO values but also reproduce the trend of the level shifting due to the covalent functionalization. For all of the QDs, the calculated optical band gap values are only 0.1 eV larger than the experimental ones, with the HOMO levels no more than 0.2 eV and the LUMO levels no more than 0.1 eV lower. The remarkable agreement, despite the simplicity of the TB model, thus establishes it as a useful tool in predicting HOMO and LUMO levels of graphene QDs and in guiding the design of QDs with desired band gaps and redox potentials. However, our previous work[16] has shown that the method, without including configuration interactions, was not sufficient in calculating the selection rules or oscillator strengths of electronic transitions observed in UV−vis absorption spectra.

We can subsequently make predictions on band gaps and redox potentials of some graphene QDs not yet synthesized. For example, with calculation, we have obtained HOMO and LUMO levels of QD **2** functionalized with an amine group at various positions (in Supporting Information). Our calculation confirmed the raising of both levels, as expected for the electron-donating amine group. Our results also revealed that the level shifting is dependent on the substitution position, highlighting the advantage of the solution-chemistry approach to graphene nanostructures in controlling their properties.

Carbon has for centuries been the largest energy supply for human society. The foreseeable depletion and the adverse environmental impact of fossil fuels call for renewable uses of carbon materials for energy. For this purpose, graphene quantum dots are very attractive because they have remarkable electro-optical properties and because the versatility of carbon chemistry enables us to fine-tune their properties. In addition, studies of well-defined, functionalized graphene quantum dots could also greatly enhance our understanding of technologically important, complex carbon materials. Here, we have demonstrated that by functionalizing the quantum dots, we can independently tune their band gaps and redox potentials, two key parameters for them to be used in energy conversion devices. By comparing the experimental values of the band gaps and redox potentials with those obtained theoretically with our TB calculation, we show that the calculation has sufficient accuracy to guide our endeavor to synthesize graphene quantum dots with desired properties.

## ■ ASSOCIATED CONTENT

**Supporting Information.** Detailed procedure for synthesis and characterization of chemical intermediates and tight-binding calculation of functionalized graphene quantum dots. This material is available free of charge via the Internet at http://pubs.acs.org.

## ■ AUTHOR INFORMATION

### Corresponding Author

*E-mail: li23@indiana.edu.

### Author Contributions

§These authors contributed equally to this work.

## ■ ACKNOWLEDGMENT

This work is supported by Indiana University, the National Science Foundation (CBET 0747751), and the ACS Petroleum Research Fund. Mass spectra were recorded at the Indiana University Mass Spectrometry Facility and NMR spectra at the Indiana University NMR Facility. We thank Dr. Yoshiyuki Nakajima at Riken Keiki Co., Ltd, for the use of a photoelectron yield spectrometer.

## ■ REFERENCES

(1) Bruchez, M.; Moronne, M.; Gin, P.; Weiss, S.; Alivisatos, A. P. Semiconductor Nanocrystals as Fluorescent Biological Labels. *Science* **1998**, *281*, 2013–2016.

(2) Chan, W. C. W.; Nie, S. M. Quantum Dot Bioconjugates for Ultrasensitive Nonisotopic Detection. *Science* **1998**, *281*, 2016–2018.

(3) Alivisatos, A. P.; Gu, W.; Larabell, C. Quantum Dots as Cellular Probes. *Annu. Rev. Biomed. Eng.* **2005**, *7*, 55–76.

(4) Klimov, V. I.; Mikhailovsky, A. A.; Xu, S.; Malko, A.; Hollingsworth, J. A.; Leatherdale, C. A.; Eisler, H. J.; Bawendi, M. G. Optical Gain and Stimulated Emission in Nanocrystal Quantum Dots. *Science* **2000**, *290*, 314–317.

(5) Eisler, H. J.; Sundar, V. C.; Bawendi, M. G.; Walsh, M.; Smith, H. I.; Klimov, V. Color-Selective Semiconductor Nanocrystal Laser. *Appl. Phys. Lett.* **2002**, *80*, 4614–4616.

(6) Huynh, W. U.; Dittmer, J. J.; Alivisatos, A. P. Hybrid Nanorod−Polymer Solar Cells. *Science* **2002**, *295*, 2425–2427.

(7) Nozik, A. J. Quantum Dot Solar Cells. *Physica E* **2002**, *14*, 115–120.

(8) Gur, I.; Fromer, N. A.; Geier, M. L.; Alivisatos, A. P. Air-Stable All-Inorganic Nanocrystal Solar Cells Processed from Solution. *Science* **2005**, *310*, 462–465.
(9) Colvin, V. L.; Schlamp, M. C.; Alivisatos, A. P. Light-Emitting-Diodes Made from Cadmium Selenide Nanocrystals and A Semiconducting Polymer. *Nature* **1994**, *370*, 354–357.
(10) Coe, S.; Woo, W. K.; Bawendi, M.; Bulovic, V. Electroluminescence from Single Monolayers of Nanocrystals in Molecular Organic Devices. *Nature* **2002**, *420*, 800–803.
(11) Tessler, N.; Medvedev, V.; Kazes, M.; Kan, S. H.; Banin, U. Efficient Near-Infrared Polymer Nanocrystat Light-Emitting Diodes. *Science* **2002**, *295*, 1506–1508.
(12) Soreni-Harari, M.; Yaacobi-ross, N.; Steiner, D.; Aharoni, A.; Banin, U.; Millo, O.; Tessler, N. Tuning Energetic Levels in Nanocrystal Quantum Dots through Surface Manipulations. *Nano Lett.* **2008**, *8*, 678–684.
(13) Shalom, M.; Ruhle, S.; Hod, I.; Yahav, S.; Zaban, A. Energy Level Alignment in CdS Quantum Dot Sensitized Solar Cells Using Molecular Dipoles. *J. Am. Chem. Soc.* **2009**, *131*, 9876–9877.
(14) Munro, A. M.; Zacher, B.; Graham, A.; Armstrong, N. R. Photoemission Spectroscopy of Tethered CdSe Nanocrystals: Shifts in Ionization Potential and Local Vacuum Level as a Function of Nanocrystal Capping Ligand. *ACS Appl. Mater. Interfaces* **2010**, *2*, 863–869.
(15) Li, L.-S.; Yan, X. Colloidal Graphene Quantum Dots. *J. Phys. Chem. Lett.* **2010**, *1*, 2572–2576.
(16) Yan, X.; Cui, X.; Li, B.; Li, L.-S. Large, Solution-Processable Graphene Quantum Dots as Light Absorbers for Photovoltaics. *Nano Lett.* **2010**, *10*, 1869–1873.
(17) Yan, X.; Cui, X.; Li, L.-S. Synthesis of Large, Stable Graphene Quantum Dots with Tunable Size. *J. Am. Chem. Soc.* **2010**, *132*, 5944–5945.
(18) Mueller, M. L.; Yan, X.; Dragnea, B.; Li, L.-S. Slow Hot-Carrier Relaxation in Colloidal Graphene Quantum Dots. *Nano Lett.* **2011**, *11*, 56–60.
(19) Pandey, A.; Guyot-Sionnest, P. Slow Electron Cooling in Colloidal Quantum Dots. *Science* **2008**, *322*, 929–932.
(20) Nozik, A. J. Quantum Dot Solar Cells. *Physica E* **2002**, *14*, 115–120.
(21) Nozik, A. J. Nanoscience and Nanostructures for Photovoltaics and Solar Fuels. *Nano Lett.* **2010**, *10*, 2735–2741.
(22) Campbell, W. M.;Highly Efficient Porphyrin Sensitizers for Dye-Sensitized Solar Cells. *J. Phys. Chem. C* **2007**, *111*, 11760–11762.
(23) De Angelis, F.; Fantacci, S.; Selloni, A.; Gratzel, M.; Nazeeruddin, M. K. Influence of the Sensitizer Adsorption Mode on the Open-Circuit Potential of Dye-Sensitized Solar Cells. *Nano Lett.* **2007**, *7*, 3189–3195.
(24) Reddy, P. Y.;Efficient Sensitization of Nanocrystalline $TiO_2$ Films by a Near-IR-Absorbing Unsymmetrical Zinc Phthalocyanine. *Angew. Chem., Int. Ed.* **2007**, *46*, 373–376.
(25) Rochford, J.; Chu, D.; Hagfeldt, A.; Galoppini, E. Tetrachelate Porphyrin Chromophores for Metal Oxide Semiconductor Sensitization: Effect of the Spacer Length and Anchoring Group Positions. *J. Am. Chem. Soc.* **2007**, *129*, 4655–4665.
(26) Serp, P.; Figueiredo, J. L. *Carbon Materials for Catalysis*; Wiley & Sons: Hoboken, NJ, 2009.
(27) Yu, D.; Nagelli, E.; Du, F.; Dai, L. Metal-Free Carbon Nanomaterials Become More Active then Metal Catalysts and Last Longer. *J. Phys. Chem. Lett.* **2010**, *1*, 2165–2173.
(28) Kamat, P. V. Graphene-Based Nanoassemblies for Energy Conversion. *J. Phys. Chem. Lett.* **2011**, *2*, 242–251.
(29) Cheng, Y.-J.; Yang, S.-H.; Hsu, C.-S. Synthesis of Conjugated Polymers for Organic Solar Cell Applications. *Chem. Rev.* **2009**, *109*, 5868–5923.
(30) Ishii, H.; Sugiyama, K.; Ito, E.; Seki, K. Energy Level Alignment and Interfacial Electronic Structures at Organic/Metal and Organic/Organic Interfaces. *Adv. Mater.* **1999**, *11*, 605–625.
(31) Schafer, J.; Ristein, J.; Ley, L.; Ibach, H. High Sensitivity Photoelectron Yield Spectroscopy with Computer-Calculated Electron Optics. *Rev. Sci. Instrum.* **1992**, *64*, 653–658.
(32) Dou, X.; Yang, X.; Bodwell, G. J.; Wagner, M.; Enkelmann, V.; Müllen, , K. Unexpected Phenyl Group Rearrangement during an Intramolecular Scholl Reaction Leading to an Alkoxy-Substituted Hexa-*peri*-hexabenzocoornene. *Org. Lett.* **2007**, *9*, 2485–2488.
(33) Wadumethrige, S. H.; Rathore, R. A Facile Synthesis of Elusive Alkoxy-Substituted Hexa-*peri*-hexabenzocoronene. *Org. Lett.* **2008**, *10*, 5139–5142.
(34) Wu, J.; Baumgarten, M.; Debije, M. G.; Warman, J. W.; Muellen, K. Arylamine-Substituted Hexa-*peri*-hexabenzocoronenes: Facile Synthesis and Their Potential Applications as "Coaxial" Hole-Transport Materials. *Angew. Chem., Int. Ed.* **2004**, *43*, 5331–5335.
(35) Bawendi, M. G.; Carroll, P. J.; Wilson, W. L.; Brus, L. E. Luminescence Properties of CdSe Quantum Crystallites: Resonance between Interior and Surface Localized States. *J. Chem. Phys.* **1992**, *96*, 946–954.
(36) Sato, R.; Dresselhaus, G.; Dresselhaus, M. S. *Physical Properties of Carbon Nanotubes*; Imperial College Press: London, 1999.
(37) Streitwieser, A., Jr. *Molecular Orbital Theory for Organic Chemists*; John Wiley & Sons: New York, 1961.